Kragujevac J. Sci. 41 (2019) 25-36. UDC 547.551:543.422.25/54:616.314
Original scientific paper

VISUALIZATION OF THE IONIZATION YIELDS MODEL OF THE NOBLE ATOMS IN AN ELLIPTICALLY POLARIZED LASER FIELD BY USING SYMBOLIC PROGRAMMING LANGUAGE

Hristina S. Delibašić*, Ivan D. Petrović and Violeta M. Petrović

University of Kragujevac, Faculty of Science, Radoja Domanovića 12, 34000 Kragujevac, Serbia
*****Corresponding author; E-mail: hristinadelibasic@gmail.com

(Received March 31st, 2019; Accepted April 30th, 2019)

ABSTRACT. In this paper, we analyzed the influence of ponderomotive and Stark shifts on the ionization yield for krypton and xenon atoms for a monochromatic wave with elliptical polarization. A brief description of the dependence of the ionization yield on the field intensity and laser wavelength is given with respect on the pulse duration and the temporal laser beam distribution. In addition, we discussed the possibility of implementing Wolfram Research technologies as a tool for generating interactive graphs based on our theoretical results. The advantage of using such plots is reflected in the fact that all calculations can be done in real time, while input parameters are manipulated with adjustable sliders, and the graphical output can be obtained almost instantaneously.

Key words: ionization yield, corrected ionization potential, Wolfram Mathematica, interactive graphics.

INTRODUCTION

Photoionization, which occurs when an atom or molecule absorbs light of sufficient energy to cause an electron to leave and create a positive ion, is behind many recent breakthroughs marking this decade of attosecond science (BUCKSBAUM, 2015). Up to now, multiple theoretical approaches (KELDYSH, 1965; REISS, 1991; AMMOSOV *et al.*, 1986) have been developed in order to understand the detailed photoionization dynamics of atoms and molecules that are exposed to the external laser field.

Based on early experimental observations, Keldysh conceived a quasistatic tunneling picture first in his 1965 paper (KELDYSH, 1965). As one of its central results, Keldysh introduced a single physical parameter - the Keldysh gamma parameter, $\gamma = \omega\sqrt{2I_p}/F$, in order to determine what regime a particular interaction belongs to. Here ω and F are the frequency and the amplitude of the laser field and I_p is unperturbed ionization potential. Generally speaking, the multiphoton regime is dominant process when $\gamma \gg 1$, while a small Keldysh parameter, $\gamma \ll 1$, corresponds to the case when quasistatic tunneling theory becomes valid. YUDIN and IVANOV (2001) suggested that for the intermediate range of the Keldysh parameter, $\gamma \sim 1$, multiphoton and tunnel ionization in strong laser fields co-exist. Additionally, according to REISS (2008), even when γ is greater than one at $\lambda = 800$ nm ionization in a strong laser field can successfully be described as a tunneling process. Unless

noted otherwise, atomic units with $e = m_e = \hbar = 1$ (MCWEENY, 1973) are adopted in this work.

After the appearance of the seminal theoretical paper by Keldysh on strong-field ionization of atoms, Ammosov-Delone-Krainov developed one of alternative model (commonly known as ADK theory) used to study the tunneling ionization of atoms (AMMOSOV *et al.*, 1986), which was also generalized to molecular systems. In the past decades, their theory is widely used to calculate the ionization rate of tunnel ionization, with a simple form of $W \propto \mathrm{Exp}\left[2\left(2I_p\right)^{3/2}/3F(t)\right]$. The exponential growth of this formula is determined primarily by the field strength, F, and the ionization potential, I_p.

An interesting aspect of photoionization processes concerns the role of laser field polarization. There are two laser field polarizations, linear and circular, as limiting cases of elliptical polarization. Most studies on the photoionization process were performed in linearly polarized laser fields, but currently the response of atoms in elliptically polarized laser fields has attracted particular attention (BUSULADŽIĆ *et al.*, 2009; LAI and DE MORISSON FARIA, 2013). Their investigation is still in demand, and the corresponding mechanism remains to be explained (HE *et al.*, 2015; KANG *et al.*, 2018; QIN *et al.*, 2019). Although great efforts have been made to explore the influence of perturbated ionization potential to the ionization dynamics for atoms subject to the elliptically polarized laser field, it is still not clear whether and how the change of potential can alter the ionization rate effectively. Wang and his coworkers in (WANG *et al.*, 2014) investigated the ellipticity dependence of the ionization yields for noble gas atoms subject to elliptically polarized laser field at 800 nm. Even with the nonadiabatic effect included, their results clearly showed the deviation of theoretical results from the measurements, where the perturbated ionization potential is totally ignored in the procedure. Their work motivated us to examine how differing the ionization potential through the Stark shift of the atomic levels and the ponderomotive potential influences the ionization yield.

This paper is organized as follows. In the next section, we reviewed the concept of the Stark shift and ponderomotive energy in strictly elliptically polarized laser field and extended it to the case of the rectangular laser beam shape. Than we discussed obtained results in the Results and the Discussion sections. After that we explained possibilities for improving our theoretical analysis using Wolfram Mathematica software. Brief summary of our work is given in conclusion section. Finally, after the acknowledgment, we gave the list of references.

THEORETICAL FRAMEWORK

In the tunneling regime, for the linearly polarized laser field, the ADK ionization rate is characterized by the following expression (AMMOSOV *et al.*, 1986):

$$W_{\mathrm{ADK}}^{\mathrm{lin}} = \frac{\left|C_{n^*l^*}\right|^2 I_p (2l+1)(l+|m|)!}{2^{|m|}|m|!(l-|m|)!}\left(\frac{2Z^3}{Fn^{*3}}\right)^{2n^*-|m|-1}\sqrt{\frac{3Fn^{*3}}{\pi Z^3}}\,\mathrm{Exp}\left(-\frac{2Z^3}{3Fn^{*3}}\right), \qquad (1)$$

where l is orbital, m magnetic, $n^* = Z/\sqrt{2I_p}$ the effective principal and $l^* = n^* - 1$ the effective orbital quantum number, Z the ion charge, $|C_{n^*l^*}|^2 = \left(2^{2n^*}\right)/(n^*\Gamma(n^* + l^* + 1)\Gamma(n^* - l^*))$ the coefficient in the asymptotic form and $\Gamma(x)$ the gamma function. The factor $\sqrt{3Fn^{*3}/\pi Z^3}$ in Eq. (1) is the result due to cycle averaging.

The ionization rate for the general case of a monochromatic wave with elliptical polarization: $F(t) = F\left(\vec{e}_x \cos\omega t + \varepsilon \vec{e}_y \sin\omega t\right)$, where ε is the ellipticity, is given by the formula (AMMOSOV *et al.*, 1986):

$$W_{\mathrm{ADK}}^{\mathrm{ellip}} = \frac{\left|C_{n^*l^*}\right|^2 I_p (2l+1)(l+|m|)!}{2^{|m|}|m|!(l-|m|)!} \sqrt{\frac{2}{\varepsilon(1+\varepsilon)}} \left(\frac{2Z^3}{Fn^{*3}}\right)^{2n^*-|m|-1} a\left(\frac{Z^3(1-\varepsilon)}{3\varepsilon F n^{*3}}\right) \mathrm{Exp}\left(-\frac{2Z^3}{3Fn^{*3}}\right), \quad (2)$$

where $a\,(x) = e^{-x} J_0(x)$ is the function in which $J_0(x)$ is the modified Bessel function of the first kind. The value of the ellipticity, ε, varied in the range $0 \leq \varepsilon \leq 1$, and for $\varepsilon = 0$ the wave is linearly, while for $\varepsilon = \pm 1$, circularly polarized.

In order to visualize the ellipticity effect, we used and modified the simple analytic formula for the normalized ionization yield. The ionization yield can be normalized at each intensity to its value for linear polarization using the approximation of the tunneling model by (WANG *et al.*, 2014):

$$Y(\varepsilon) = \frac{W_{\mathrm{ADK}}^{\mathrm{ellip}}}{W_{\mathrm{ADK}}^{\mathrm{lin}}} = \frac{\left|C_{n^*l^*}\right|^2 I_p \frac{(2l+1)(l+|m|)!}{2^{|m|}|m|!(l-|m|)!} \left(\frac{2Z^3}{Fn^{*3}}\right)^{2n^*-|m|-1} \left(\frac{\varepsilon(1+\varepsilon)}{2}\right)^{-\frac{1}{2}} a\left(\frac{1-\varepsilon}{3\varepsilon}\frac{Z^3}{Fn^{*3}}\right) \mathrm{Exp}\left(-\frac{2Z^3}{3Fn^{*3}}\right)}{\left|C_{n^*l^*}\right|^2 I_p \frac{(2l+1)(l+|m|)!}{2^{|m|}|m|!(l-|m|)!} \left(\frac{2Z^3}{Fn^{*3}}\right)^{2n^*-|m|-1} \left(\frac{3Fn^{*3}}{\pi Z^3}\right)^{1/2} \mathrm{Exp}\left(-\frac{2Z^3}{3Fn^{*3}}\right)}. \quad (3)$$

After some simple mathematical manipulations, the Eq. (3) can be written as:

$$Y(\varepsilon) = \left(\frac{3Fn^{*3}}{\pi Z^3}\frac{\varepsilon(1+\varepsilon)}{2}\right)^{-1/2} a\left(\frac{1-\varepsilon}{3\varepsilon}\frac{Z^3}{Fn^{*3}}\right). \quad (4)$$

Substituting the definition of effective principal quantum number, n^*, in Eq. (4), and for case of single ionized atom, we obtained:

$$Y(\varepsilon) = \left(\frac{3F\varepsilon(1+\varepsilon)}{2\pi(2I_p)^{3/2}}\right)^{-1/2} a\left(\frac{1-\varepsilon}{3\varepsilon}\frac{(2I_p)^{3/2}}{F}\right), \quad (5)$$

where $a(x)$ is a monotonically decreasing function, $a\,(x) = e^{-x} J_0(x)$, in which part with modified Bessel function of the first kind, $J_0(x)$, can be approximate as: $J_0(x) \approx 1/\sqrt{2\pi x}$ (LUKE, 2014). Now, Eq. (5) can be, after some simple manipulation, written in the following form:

$$Y(\varepsilon) = (1-\varepsilon^2)^{-1/2} \,\mathrm{Exp}\left(\frac{1-\varepsilon}{3\varepsilon}\frac{(2I_p)^{3/2}}{F}\right) \approx \mathrm{Exp}\left[-\frac{(2I_p)^{\frac{3}{2}}}{3F}\varepsilon^2\right]. \quad (6)$$

The Eq. (6) explicitly indicates that the ionization yield, $Y(\varepsilon)$, decreases exponentially with increasing ellipticity, ε, and the ionization potential, I_p. In the standard perturbative approach, it is shown that the intense laser field influences the electron's binding potential, perturbs it and makes it much higher than the unperturbed value. There are at least two reasons for this increase: the Stark shift and ponderomotive potential (VOLKOVA *et al.*, 2011; PROTOPAPAS *et al.*, 1997). Atom's energy levels are altered in the laser field and this effect is known as the Stark effect. This displacement of the energy level is determined by expression $I_{st} = \frac{\alpha_p f_2(t) F^2}{2} + \frac{\gamma_h f_4(t) F^4}{24}$ (MAROULIS, 2006), in which α_p is the dipole polarizability, γ_h is the dipole hyperpolarizability and functions $f_2(t)$, $f_4(t)$ are the slowly varying pulse envelope determined by the laser pulse envelope and central radiation frequency ω. For the special case of a static field, these functions are equal: $f_2(t) = f_4(t) = 1$ (KORNEV *et al.*, 2014). The values of polarizability, α_p, and hyperpolarizability, γ_h, for different atoms and ions can be found in (MAROULIS, 2006; SHELTON, 1990). Additionally, the average oscillation kinetic energy of a free electron is represented as the ponderomotive potential and in the electric field

of the laser with strength, F, for elliptically polarized laser field, is given by the formula: $U_p = \frac{F^2(1+\varepsilon^2)}{4\omega^2}$ (PAULUS *et al.*, 1998). The ponderomotive potential causes a shift of the atomic energies respectively to the continuum (RUPP, 2016).

Having both effects in mind, we can write the corrected ionization potential, I_p^{eff}, in the following form (VOLKOVA *et al*, 2011):

$$I_p^{eff}(\varepsilon) = I_p + U_p + I_{st} = I_p + \frac{F^2(1+\varepsilon^2)}{4\omega^2} + \frac{\alpha_p F^2}{2} + \frac{\gamma_h F^4}{24}. \quad (7)$$

In order to analyze how the ionization yield, $Y(\varepsilon)$, is affected by corrected ionization potential, I_p^{eff}, we substituted unperturbed ionization potential, I_p, with the shifted, the corrected effective ionization potential, I_p^{eff} in Eq. (6) and obtained the following expression:

$$Y_{corr}(\varepsilon) \approx \mathrm{Exp}\left[-\frac{\left(2\left(I_p+\frac{F^2(1+\varepsilon^2)}{4\omega^2}+\frac{\alpha_p F^2}{2}+\frac{\gamma_h F^4}{24}\right)\right)^{3/2}}{3F}\varepsilon^2\right]. \quad (8)$$

where $Y_{corr}(\varepsilon)$ denotes the corrected tunneling ionization yield for elliptical polarization of the laser field.

The laser beam shaping is one of the most important factors that influence the ionization yield, because no matter how fast the ionization process occurs, it is governed by the laser field strength. The purpose of changing beam shape is to examine how differing the pulse envelope $F(t)$, the laser frequency ω, and the pulse duration t influences the ionization yield (BAUER, 1999). On the other hand, the change of a beam shape in experimental environment may provide evidence for a future theory to explain. There are many different shapes and here we wanted to discuss how, the choice of some particular shape, influences the yield.

We considered the case of a rectangular laser beam shape, F_R, with central frequency ω and with a femtosecond pulse duration in the form (RHEE *et al.*, 1996):

$$F_R(t) = F \sin \omega t. \quad (9)$$

This type of beam shape is often used in modern high-power lasers beam shapers and it is beneficial for many applications in which the laser beam is being focused to a small spot (TANIGUCHI *et al* 2013). Functions $f_2(t)$ and $f_4(t)$, which we already defined, for the rectangular pulse, became: $f_2(t) = \frac{1}{2}$ and $f_4(t) = \frac{3}{8}$ (KORNEV *et al.*, 2014). Also, the additional terms which can be seen in the Eq. (3), compared to the Eq. (1), directly depends on the field strength, F. The replacement of F by $F_R(t)$, i.e. modulation of generally assumed laser beam shape, F, with the rectangular laser beam shape, $F_R(t)$, in Eq. (8) allows us to examine a dependence of the ionization yield on the laser beam shape.

The Stark shift averaged over the optical cycle for the case of the rectangular pulse has the following form: ${I_{st}}^R(t) = \frac{\alpha_p F_R(t)^2}{4} + \frac{\gamma_h F_R(t)^4}{64}$ while the ponderomotive potential, U_p, remains unchanged, $U_p(t) = \frac{F_R(t)^2(1+\varepsilon^2)}{4\omega^2}$. Now, the corrected ionization potential, for the rectangular laser pulse, can be written as:

$$I_p^{eff,R}(\varepsilon, t) = I_p + U_p^R(t) + I_{st}^R(t) = I_p + \frac{F_R(t)^2(1+\varepsilon^2)}{4\omega^2} + \frac{\alpha_p F_R(t)^2}{4} + \frac{\gamma_h F_R(t)^4}{64}. \quad (10)$$

Next, we incorporated the laser beam shape from Eq. (9) and corrected ionization potential, $I_p^{eff,R}(t)$ (Eq. (10)) in the formula for the ionization yield (Eq. (6)), and obtained:

$$Y_{corr,R}(\varepsilon,t) \approx \mathrm{Exp}[-\frac{\left(2\left(I_p+\frac{F_R(t)^2(1+\varepsilon^2)}{4\omega^2}+\frac{\alpha_p F_R(t)^2}{4}+\frac{\gamma_h F_R(t)^4}{64}\right)\right)^{3/2}}{3F_R(t)}\varepsilon^2]. \quad (11)$$

Regard to the initial formula (Eq. (6)) it can be seen that the dependence is kept, but time-dependent laser field $F_R(t)$ and fully corrected ionization potential, gives us an additional possibility to analyze the behavior of the ionization yield for an elliptically polarized field.

RESULTS AND DISCUSSION

In this section we theoretically investigated the ellipticity-dependent ionization yield of krypton (Kr) and xenon (Xe) atoms ionized by a laser of $\lambda = 800$ nm wavelength. Field intensities, I, used in the present study have been varied within the range: $I = 1 \times 10^{14} - 1 \times 10^{16}$ W/cm^2 with pulse duration of $\tau = 10$ fs. These parameters limited the value of the Keldysh parameter in the range which is characteristic for the tunnel ionization. The ellipticity varied in the range $\varepsilon(0,1)$. We assumed the rectangular beam profile with, step by step, included fully corrected ionization potential.

First, we plotted the ionization yield, based on Eq. (11), as a function of the field intensity, I (2D graph) and both, the field intensity, I, and the ellipticity, ε, (3D graph). In order to analyze the influence of the ponderomotive and Stark shift effects on the ionization yield, we included them sequentially. In Fig. 1, we displayed comparative review of the yields of Kr atom with the unperturbated, with the ponderomotive and fully corrected ionization potential. The marks in subscript denote the included ponderomotive potential (U_p) and Stark shift (I_{st}) in the ionization yield.

In Fig. 1(a) we started with the ellipticity, $\varepsilon = 0.25$, i.e. with the case of a near linearly polarized laser field. All observed theoretical curves, $Y(\varepsilon,t)$, $Y_{U_p}(\varepsilon,t)$ and $Y_{U_p,I_{st}}(\varepsilon,t)$, in the low laser intensity regime exhibit identical behavior, but for higher intensities we observe significant differences in curve flow. The curve which includes the influence of the ponderomotive potential, $Y_{U_p}(\varepsilon,t)$, (green line in Fig. 1(a)) have almost the same "flow" as a curve with uncorrected ionization potential, $Y(\varepsilon,t)$, (red line in Fig. 1(a)). Both increase monotonically from zero and reach a slowly rising plateau around the laser intensity $I = 6 \times 10^{15}$Wcm^{-2}. The appearance of the plateau is due to the fact that maximum number of photoelectrons is ejected under the observed conditions (MILADINOVIĆ and PETROVIĆ, 2016). Additionally, with the intensity increasing, there is a significant deviation of the curve with fully corrected ionization potential, $Y_{U_p,I_{st}}(\varepsilon,t)$, which is completely in accordance with the theoretical predictions (DELONE and KRAINOV, 1998). Our observation shows that, in spite of fact that is commonly neglected, the ionization yield is very influenced by inclusion of the Stark shift and ponderomotive potential.

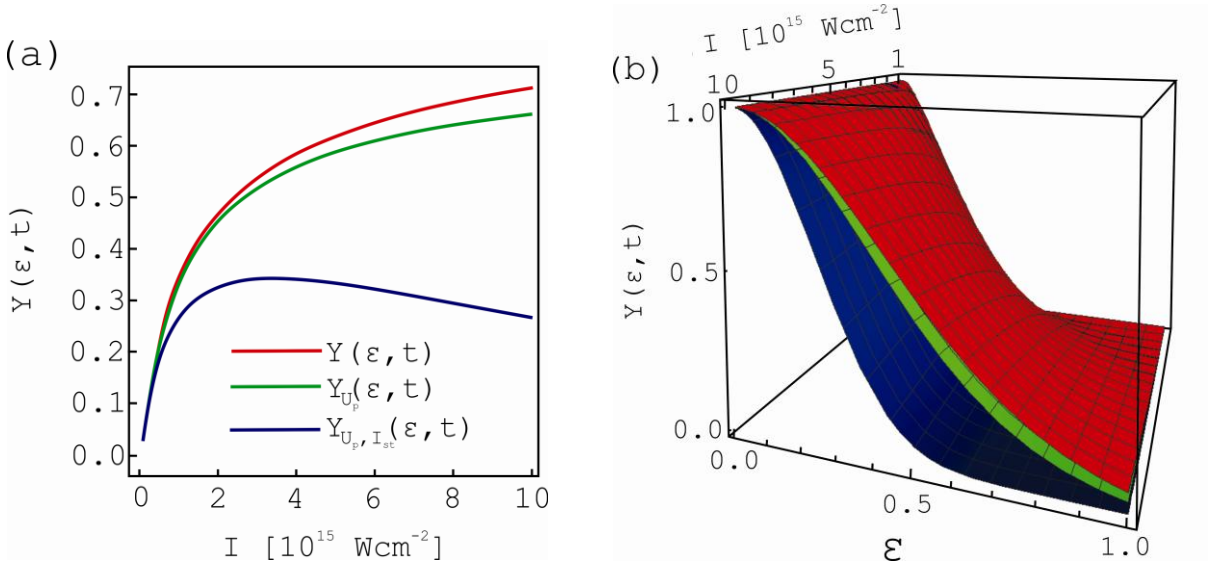

Figure 1. Comparative review of the ionization yields $Y(\varepsilon,t)$, $Y_{U_p}(\varepsilon,t)$ and $Y_{U_p,I_{st}}(\varepsilon,t)$, for Kr atom as a function of laser field intensity, $I = 1\times10^{14} - 1\times10^{16}$ Wcm^{-2}, when ellipticity: (a) is fixed to the value $\varepsilon = 0.25$, (b) varies within the range $\varepsilon(0,1)$.

Results illustrated in Fig. 1(b) suggests that for $\varepsilon > 0.4$ inclusion of the mentioned effect causes a sudden decrease of the yield with fully corrected ionization potential, $Y_{U_p,I_{st}}(\varepsilon,t)$, as well as a shift through the lower ellipticities. This is completely expected, because the experimental results in (SUN *et al.*, 2018) implied that for the higher values of ellipticity the electron reaches the detector directly after the tunneling ionization without further interaction with the core, and hence, the probability of the electron being captured by the ionic core in strong laser fields is negligible. In addition, for $\varepsilon > 0.2$, the ionization yield curve which corresponds to the case of fully corrected ionization potential $Y_{U_p,I_{st}}(\varepsilon,t)$, deviates noticeably from yields, $Y(\varepsilon,t)$ and $Y_{U_p}(\varepsilon,t)$. According to the ionization picture in (RICHTHER *et al.*, 2016), for value of $\varepsilon < 0.2$, the ionized electron can return to the core and may be captured again by the core, resulting in the ionization suppression. Thus, the ionization yield for linear polarization may be overestimated. Our results are in good agreement with the experimental observations (SUN *et al.*, 2018; WANG *et al.*, 2014). This implies that the semiclassical model can be applied to understand the nature of photoionization process under the elliptically polarized laser field.

In the following, we study the laser wavelength (frequency) dependence of the ionization yield of Xe atom with different ellipticities. Results are displayed in Fig. 2.

One can read from the Fig. 2 that all curves first increase, reach a peak, and then drop with increasing wavelength (decreasing frequency). It is noteworthy that the value and position of the peak depend on ellipticity. For $\varepsilon = 0.65$, $\varepsilon = 0.70$ and $\varepsilon = 0.75$ it appears at 565.85 nm, 576.25 nm, and 587.23 nm, respectively. An increase of ellipticity makes the yield reach a peak at a higher wavelength. Obviously, the maximal value that the curves can reach increases with ellipticity. A closer inspection of Fig. 2 clearly shows that lower values of ellipticity contribute to increasing of the ionization yield value. Additionally, lines with different ellipticities coincide with each other in the short-wavelength regime. This fact can be explained using the mechanism used to describe the frequency dependence in (CHEN *et al.*, 2003).

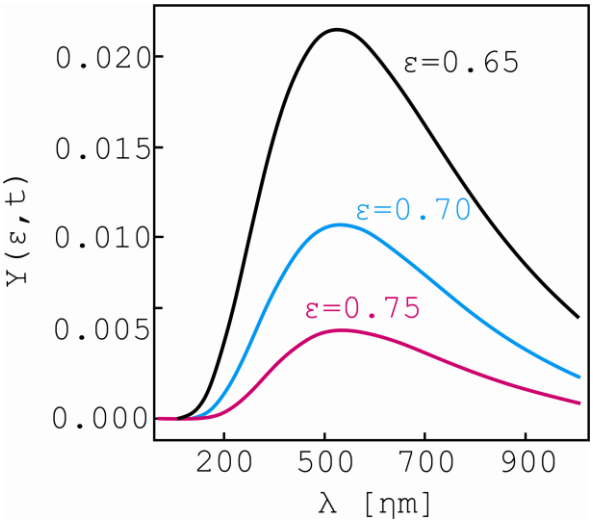

Figure 2. Wavelength dependence of the fully corrected ionization yield, $Y_{U_p,I_{st}}(\varepsilon,t)$, for the ellipticity $\varepsilon = 0.65, 0.70, 0.75$. In order from top to bottom: black curve $\varepsilon = 0.65$, blue curve $\varepsilon = 0.70$ and magenta curve $\varepsilon = 0.75$. Intensity is fixed to the value $I = 1 \times 10^{15}$ Wcm^{-2}, while laser wavelength varies within the range: $\lambda = 100 - 1100$ nm.

Our results also showed that when the wavelength increases the yield begins to saturate and then decreases with wavelength. This behavior is in accordance with (CHEN *et al.*, 2003, WIEHLE, 2005). In addition, our calculation clearly showed that when the ellipticity increases further value ionization yield significantly reduces.

WOLFRAM LANGUAGE

A computer algebra software can be used to improve theoretical analysis in different scientific area, such as physics, chemistry, material science and software engineering. In most of these areas, it is necessary to operate over a wide range of scales in order to visualize functions, equations and inequalities and analyze obtained results. Such multiscale modeling usually operates with different phenomena and it is currently one of the hot topics in theoretical and experimental research (MACCALLUM, 2018; SHYSHKINA *et al.*, 2018).

Extensive research has been done on finding comprehensive mathematical analysis system which suits both theoretical development and extensive data analysis (KARIMI *et al.* 2018; GADKARI *et al.*, 2018). To achieve this goal, in the preset paper, we used program *Wolfram Mathematica* (WOLFRAM, 1999) for all research tasks without having to change software for different subtasks. Other packages keep subdividing as new features are added, but *Mathematica* gets moreover unified as benefits modern research (KRISTALINSKII and CHERNYI, 2019). Additionally, we would like to note that it can be very powerful tool which can be used to visualize and display wide range of physics concepts and to generate numerical and graphical solutions to physics problems. This is why it plays an important role in theoretical physics.

Version 7.0 of *Mathematica* introduced function **Manipulate [ ]** which allows for the manual adjustment of variable parameters through the use of sliders and buttons. In this way, the creation of interactive graphics are greatly simplified. For example, the Mathematica code to generate plots of ionization yield with the unperturbated, $Y(\varepsilon,t)$, and fully corrected ionization potential, $Y_{U_p,I_{st}}(\varepsilon,t)$, based on Eq. (11) is shown with the program output in Fig. 3.

```
Manipulate[
 Module[{Ip = 0.514475937, c = 137},
  Plot[
   {Exp[
     -((2 * Ip + (F[Int] * Sin[(c/λ * 2 * Pi) * t])^2 * (1 + ε^2)/(4 * (c/λ * 2 * Pi)^2) + 1/2 * 16.08 * (F[Int] * Sin[(c/λ * 2 * Pi) * t])^2 + 3/(4 * 24) * 2600 * (F[Int] * Sin[(c/λ * 2 * Pi) * t])^4)^(3/2)/
      (3 * (F[Int] * Sin[(c/λ * 2 * Pi) * t])) * ε^2], Exp[-((2 * Ip)^(3/2) * ε^2)/(3 * F[Int] * Sin[(c/λ * 2 * Pi) * t])]}, {Int, 1 * 10^14, 1 * 10^16},
   PlotRange → {All, {0.8, 1}},
   AxesOrigin → {500, 0},
   ImageSize → {600, 300},
   Frame → True,
   FrameLabel → {{HoldForm["Y(ε,t)"], None}, {HoldForm["I[Wcm^-2]"], None}},
   LabelStyle → {FontSize → 20},
   PlotStyle → {Blue, Red}, PlotLegends → Placed[LineLegend[{"perturbated ionization yield", "unperturbated ionization yield"},
      LabelStyle → {FontSize → 16},
      LegendMarkerSize → 40], Above]]],
 {{λ, 3779.45, "laser wavelength"}, 3779.45, 37794.51, Appearance → "Labeled"},
 {{ε, 0, "ellipticity"}, 0, 1, 0.01, Appearance → "Labeled"},
 TrackedSymbols :> {λ, ε}]
```

Figure 3. *Mathematica* code to produce an interactive plot for $Y(\varepsilon, t)$ and $Y_{U_p, I_{st}}(\varepsilon, t)$ based on Eq. (11) for the case of Kr atom.

The fourth and fifth line of code represented in Fig. 3 plots Eq. (11) as a function of laser field intensity, I, the range , $I = 1 \times 10^{14} - 1 \times 10^{16}$ Wcm^{-2}. The lines of code immediately above and below adjust the values of the laser wavelength, λ, unperturbated ionization potential, I_p, speed of light, c, and pulse duration, τ, in atomic units (McWeeny, 1973) as well as font type and size, axis labels, figure labels, annotations, and legends. It is obvious that most of the code consists of formatting options for the plot and only a few lines of code are needed to create the sliders allowing manual adjustment of the variables λ and ε. Additionally, we would like to note that simulations which are numerical solutions to sets of differential equations are also relatively easy to prepare (Gray *et al.*, 1997).

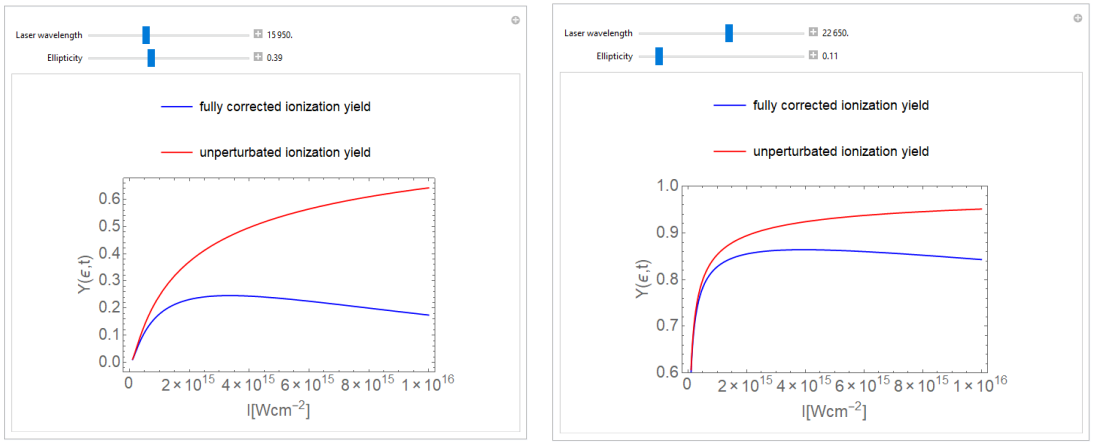

Figure 4. Laser field intensity dependence of the fully corrected ionization yield, $Y_{U_p, I_{st}}(\varepsilon, t)$ for Kr atom. Moving the sliders adjusts the ellipticity, ε, and the laser wavelength, λ.

We demonstrated in Fig. 4 output of the *Mathematica* code based on Fig. 3. The sliders allow the user to immediately change values of the ellipticity, ε, the field intensity, I, and pulse duration, τ, and continuously update the obtained plot for ionization yield based on Eq. (11).

In order to more fully explore the dependence of Eq. (11) on observed variables, one could use an interactive 3D plot as shown in Fig. 5. Here, the ionization yield is plotted as a function of the ellipticity, ε, and the wavelength, λ. Moving the field intensity, I, slider allows

the user to see how the ionization yield, $Y(\varepsilon, t)$ and $Y_{U_p, I_{st}}(\varepsilon, t)$, curves changes with the ellipticity, ε, and the wavelength, λ.

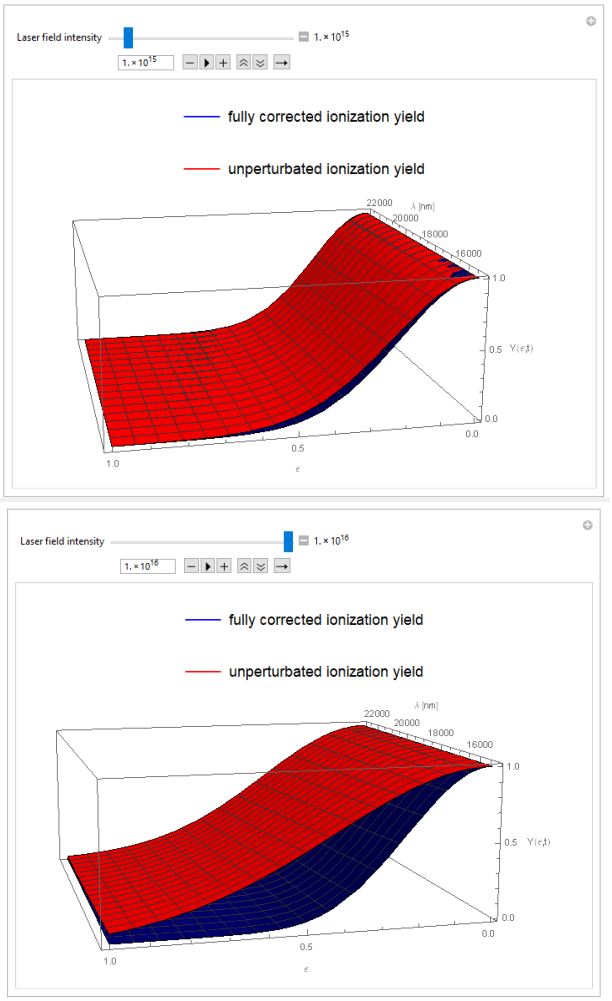

Figure 5. Two screen captures of an interactive Mathematica interactive plot showing the fully corrected ionization yield, $Y_{U_p, I_{st}}(\varepsilon, t)$ as a function of the ellipticity $\varepsilon(0,1)$ and laser wavelength $\lambda = 800 - 1200$ nm (1 nm $=$ 18.89 a. u.) for the case of Xe atom, with a slider that allows the viewer to adjust the laser field intensity, I.

A closer inspection of Fig. 5 clearly indicates that higher values of the field intensity, I, contribute to increase of the ionization yields. An interactive plot like this can allow the user to extract a numerical value, but it also allows for a graphical exploration of a complicated system of equations in an accessible manner. Additionally, interactive plot illustrated in Fig. 5 permits the user to enter the numerical values of the field intensity directly. This version is easy for simply and quickly obtaining results.

CONCLUSION

The theory presented in this paper provides an efficient theoretical model for calculating the ionization yields of krypton and xenon atoms. Described theoretical model can be extended to other noble gas atoms, which can further test the validity of the present theory. In our analysis we were interested to examine and to discuss how change of the ellipticity, ε, laser wavelength, λ, and the field intensity, I, contributes ionization yields. Because of that we provided several examples of interactive plots, which were created in *Mathematica.* The

results presented in this paper undoubtedly showed that a minimal change of the mentioned parameters strongly affects the ionization yield.

Acknowledgments

The authors are grateful to the Serbian Ministry of Education, Science and Technological Development for financial support through Project 171020.

References:

[1] AMMOSOV, M.V., DELONE, N.B., KRAINOV, V.P. (1986): Tunnel Ionization of Complex Atoms and of Atomic Ions in an Alternating Electric Field. *Soviet Physics JETP* **64**(6): 1191-1194.

[2] BAUER, D., MULSER, P. (1999): Exact field ionization rates in the barrier-suppression regime from numerical time-dependent Schrödinger-equation calculations. *Physical Review A* **59**(1): 569. doi:10.1103/PhysRevA.59.569

[3] BUCKSBAUM, P.H. (2015): Sources and Science of Attosecond Light. *Optics and Photonics News* **26**(5): 28-35. doi:10.1364/OPN.26.5.000028

[4] BUSULADŽIĆ, M., GAZIBEGOVIĆIĆ-BUSULADŽIĆ, A., MILOŠEVIĆ, D.B. (2009): Strong-field approximation for ionization of a diatomic molecule by a strong laser field. III. High-order above-threshold ionization by an elliptically polarized field. *Physical Review A* **80**(1): 013420. doi:10.1103/PhysRevA.80.013420

[5] CHEN, J., KIM, J.H., NAM, C.H. (2003): Frequency dependence of non-sequential double ionization. *Journal of Physics B: Atomic, Molecular and Optical Physics* **36**(4): 691-697. doi: 10.1088/0953-4075/36/4/303

[6] DELONE, N.B., KRAINOV, V.P. (1998): Tunneling and barrier-suppression ionization of atoms and ions in a laser radiation field. *Physics-Uspekhi* **41**: 469-485.

[7] GADKARI, S., GU, S., SADHUKHAN, J. (2018): Towards automated design of bio electrochemical systems: A comprehensive review of mathematical models. *Chemical Engineering Journal* **343**: 303-316. doi:10.1016/j.cej.2018.03.005

[8] MAROULIS, G. (2006): Atoms, Molecules and Clusters in Electric Fields: Theoretical Approaches to the calculation of electric polarizability (Vol. 1). *World Scientific* doi: 10.1142/p464

[9] GRAY, A., MEZZINO, M., PINSKY, M.A. (1997): *Introduction to ordinary differential equations with Mathematica: an integrated multimedia approach*. Springer.

[10] HE, P.L., TAKEMOTO, N., HE, F. (2015): Photoelectron momentum distributions of atomic and molecular systems in strong circularly or elliptically polarized laser fields. *Physical Review A* **91**(6): 063413. doi:10.1103/PhysRevA.91.063413

[11] KANG, H., HENRICHS, K., KUNITSKI, M., WANG, Y., HAO, X., FEHRE, K., JAHNKE, T. (2018): Timing Recollision in Nonsequential Double Ionization by Intense Elliptically Polarized Laser Pulses. *Physical review letters* **120**(22): 223204. doi: 10.1103/PhysRevLett.120.223204

[12] KARIMI, R., GHEINANI, T.T., AVARGANI, V.M. (2018): A detailed mathematical model for thermal performance analysis of a cylindrical cavity receiver in a solar parabolic dish collector system. *Renewable energy* **125**: 768-782. doi:10.1016/j.renene.2018.03.015

[13] KELDYSH, L.V. (1965): Ionization in the field of a strong electromagnetic wave. *Soviet Physics JETP* **20**(5): 1307-1314.

[14] KORNEV, A.S., SEMILETOV, I.M., ZON, B.A. (2014): Keldysh theory in a few-cycle laser pulse, inelastic tunneling and Stark shift: comparison with ab initio calculation. *Journal of Physics B: Atomic, Molecular and Optical Physics* **47**(20): 204026. doi:10.1088/0953-4075/47/20/204026

[15] KRISTALINSKII, V.R., CHERNYI, S.N. (2019): On solving dynamic programming problems in the Wolfram Mathematica system. *International Journal of Open Information Technologies* **7**(2): 42-48.

[16] LAI, X., DE MORISSON FARIA, C.F. (2013): Temporal and spatial interference in molecular above-threshold ionization with elliptically polarized fields. *Physical Review A* **88**(1): 013406. doi:10.1103/PhysRevA.88.013406

[17] LUKE, Y.L. (2014): *Integrals of Bessel functions*. Dover publications Inc, New York.

[18] MACCALLUM, M.A.H. (2018): Computer algebra in gravity research. *Living reviews in relativity* **21**(6):1-93. doi:10.1007/s41114-018-0015-6

[19] MCWEENY, R. (1973): Natural units in atomic and molecular physics. *Nature* **243**(5404): 196-198. doi: 10.1038/243196a0

[20] MILADINOVIĆ, T.B., PETROVIĆ, V.M. (2016): Behaviour of tunnelling transition rate of argon atom exposed to strong low-frequency elliptical laser field. *Pramana* **86**(3): 565-573.

[21] PAULUS, G.G., ZACHER, F., WALTHER, H., LOHR, A., BECKER, W., KLEBER, M. (1998): Above-threshold ionization by an elliptically polarized field: quantum tunneling interferences and classical dodging. *Physical review letters* **80**(3): 484-487. doi: 10.1103/PhysRevLett.80.484

[22] PROTOPAPAS, M., KEITEL, C.H., KNIGHT, P.L. (1997): Atomic physics with super-high intensity lasers. *Reports on Progress in Physics* **60**(4): 389-486.

[23] QIN, Y. N., LI, M., LI, Y., HE, M., LUO, S., LIU, Y., LU, P. (2019): Asymmetry of the photoelectron momentum distribution from molecular ionization in elliptically polarized laser pulses. *Physical Review A* **99**(1): 013431. doi:10.1103/PhysRevA.99.013431

[24] REISS, H.R. (1991): Strong-field approximation in photoionization. *Radiation Effects and Defects in Solids* **122**(2): 693-710.

[25] REISS, H.R. (2008): Limits on tunneling theories of strong-field ionization. *Physical review letters* **101**(4): 043002. doi:10.1103/PhysRevLett.101.043002

[26] RHEE, J.K., SOSNOWSKI, T.S., TIEN, A.C., NORRIS, T.B. (1996): Real-time dispersion analyzer of femtosecond laser pulses with use of a spectrally and temporally resolved up conversion technique. *JOSA B* **13**(8): 1780-1785.

[27] RICHTHER, M., KUNITSKI, M., SCHOFFLER, M., JAHNKE, T., SCHMIDT, L. P. H., DORNER, R. (2016): Ionization in orthogonal two-color laser fields: Origin and phase dependences of trajectory-resolved Coulomb effects. *Physical Review A* **94** (3): 033416. doi: 10.1103/PhysRevA.94.033416

[28] RUPP, D. (2016): *Ionization and plasma dynamics of single large xenon clusters in superintense XUV pulses*. Springer.

[29] SHELTON, D.P. (1990): Nonlinear-optical susceptibilities of gases measured at 1064 and 1319 nm. *Physical Review A* **42**(5): 2578.

[30] SHYSHKINA, M., KOHUT, U., POPEL, M. (2018): The Systems of Computer Mathematics in the Cloud-Based Learning Environment of Educational Institutions. *Proceedings of the 12th International Conference on ICT in Education, Research and Industrial Applications. Integration, Harmonization and Knowledge Transfer* (ICTERI, 2017). arXiv preprint arXiv:1807.01770.

[31] SUN, R., LAI, X., QUAN, W., YU, S., WANG, Y., XU, S., LIU, X. (2018): Coulomb potential effects in strong-field atomic ionization under elliptical polarization. *Physical Review A* **98**(5): 053418. doi:10.1103/PhysRevA.98.053418

[32] TANIGUCHI, J., ITO, H., MIZUNO, J., SAITO, T. (eds.). (2013): *Nanoimprint technology: nanotransfer for thermoplastic and photocurable polymers*. John Wiley & Sons.

[33] VOLKOVA, E.A., POPOV, A.M., TIKIHONOVA, O.V. (2011): Ionization and stabilization of atoms in a high-intensity, low-frequency laser field. *Journal of Experimental and Theoretical Physics* **113**: 394-406.

[34] WANG, C., LAI, X., HU, Z., CHEN, Y., QUAN, W., KANG, H., LIU, X. (2014): Strong-field atomic ionization in elliptically polarized laser fields. *Physical Review A* **90**(1): 013422. doi: 10.1103/PhysRevA.90.013422

[35] WIEHLE, R. (2005): Experimental examination of ionization processes of noble gases in strong laser fields (Doctoral dissertation).

[36] WOLFRAM, S. (1999): *The mathematica book.* Cambridge university press.

[37] YUDIN, G.L., IVANOV, M.Y. (2001): Nonadiabatic tunnel ionization: Looking inside a laser cycle. *Physical Review A* **64**(1): 013409.